

# HIV infection changes glomerular podocyte cytoskeletal composition and results in distinct cellular mechanical properties

R. Tandon, I. Levental, C. Huang, F. J. Byfield, J. Ziembicki, J. R. Schelling, L. A. Bruggeman, J. R. Sedor, P. A. Janmey and R. T. Miller

*Am J Physiol Renal Physiol* 292:F701-F710, 2007. First published 17 October 2006;  
doi: 10.1152/ajprenal.00246.2006

## You might find this additional info useful...

---

This article cites 38 articles, 18 of which you can access for free at:  
<http://ajprenal.physiology.org/content/292/2/F701.full#ref-list-1>

This article has been cited by 3 other HighWire-hosted articles:  
<http://ajprenal.physiology.org/content/292/2/F701#cited-by>

Updated information and services including high resolution figures, can be found at:  
<http://ajprenal.physiology.org/content/292/2/F701.full>

Additional material and information about *American Journal of Physiology - Renal Physiology* can be found at:  
<http://www.the-aps.org/publications/ajprenal>

---

This information is current as of September 7, 2012.

*American Journal of Physiology - Renal Physiology* publishes original manuscripts on a broad range of subjects relating to the kidney, urinary tract, and their respective cells and vasculature, as well as to the control of body fluid volume and composition. It is published 12 times a year (monthly) by the American Physiological Society, 9650 Rockville Pike, Bethesda MD 20814-3991. Copyright © 2007 the American Physiological Society. ISSN: 0363-6127, ESN: 1522-1466. Visit our website at <http://www.the-aps.org/>.

## HIV infection changes glomerular podocyte cytoskeletal composition and results in distinct cellular mechanical properties

R. Tandon, I. Levental, C. Huang, F. J. Byfield, J. Ziembicki, J. R. Schelling,  
L. A. Bruggeman, J. R. Sedor, P. A. Janmey, and R. T. Miller

Departments of Surgery and Medicine, Case Western Reserve University, Louis Stokes Veterans  
Affairs Medical Center, Rammekamp Center for Research, MetroHealth Medical Center, Cleveland, Ohio;  
and Departments of Physiology and Bioengineering, University of Pennsylvania, Philadelphia, Pennsylvania

Submitted 30 June 2006; accepted in final form 3 October 2006

**Tandon R, Levental I, Huang C, Byfield FJ, Ziembicki J, Schelling JR, Bruggeman LA, Sedor JR, Janmey PA, Miller RT.** HIV infection changes glomerular podocyte cytoskeletal composition and results in distinct cellular mechanical properties. *Am J Physiol Renal Physiol* 292: F701–F710, 2007. First published October 17, 2006; doi:10.1152/ajprenal.00246.2006.—In addition to forming the selective filtration barrier for the renal glomerulus, podocytes maintain glomerular capillary architecture by opposing distending hemodynamic forces. To understand the relationship of cytoskeletal properties and the mechanical characteristics of podocytes, we studied filamin expression and distribution and measured cell membrane deformability in conditionally immortalized wild-type (WT) mouse podocytes, and in podocytes derived from a mouse model of HIV-associated nephropathy (HIVAN). In the WT cells, filamin and F-actin were localized at the periphery and in prominent stress fibers. In the HIVAN cells, filamin expression was reduced, and stress fibers were sparse. In a microaspiration assay, HIVAN cells ruptured under minimal negative pressure. Atomic force microscopy demonstrated that the WT cells had a stiffness of 17 kPa, whereas the value for the HIVAN cells was 4 kPa. These results demonstrate that the mechanical properties of WT and HIVAN podocytes are markedly different in a manner that is consistent with differences in the composition and arrangement of their cytoskeletons. The mechanical properties of the WT podocytes suggest that these cells can better maintain capillary integrity than the HIVAN podocytes and implicate pathological assembly of the cytoskeleton as a mechanism of HIVAN.

elasticity; membrane

PODCYTES ARE TERMINALLY DIFFERENTIATED cells that comprise the outer layer of the glomerular capillary. Their specialized slit diaphragms form the filtration barrier for the glomerulus and they provide mechanical support to oppose the hemodynamic forces from blood flow through the capillaries. Disease states such as diabetes and hypertension are characterized by glomerular hyperfiltration with increased glomerular capillary pressures and flows that expose podocytes to increased mechanical force. In several experimental models, the increased hemodynamic forces result in podocyte injury and loss, dilation of capillaries, and ultimately focal segmental glomerulosclerosis (FSGS) that progresses to glomerular obsolescence (19, 27, 28). In contrast to most other genetically defined forms of FSGS, HIV-associated nephropathy (HIVAN) is an acquired disease that begins in structurally normal podocytes as a consequence of their infection with the HIV virus (3, 5, 42). HIVAN is associated with a variant of FSGS characterized by

apparent collapse of the glomerulus and capillaries (collapsing variant of FSGS) and dedifferentiation of the podocytes (3). We propose that abnormalities in podocyte cytoskeletal assembly impair their ability to regulate capillary structure in response to hemodynamic forces. Since cultured HIVAN podocytes retain many properties of native HIV-infected podocytes and represent a reproducible disease model, we chose to compare aspects of their cytoskeletal structure and mechanical properties in an effort to determine whether these characteristics were altered in a manner that could contribute to disease (3, 5, 42).

The composition and organization of the actin cytoskeleton are the principal determinants of the mechanical properties of cells, but podocytes are relatively uncharacterized in these respects. The physical characteristics of filamentous actin in the cytoskeleton (cortical actin and stress fibers) are dependent on the level of expression and localization of actin bundling and cross-linking proteins such as filamin and  $\alpha$ -actinin. Filamentous actin networks alone, or those nucleated from branches of the ARP2/3 complex, have relatively little structural integrity (13, 29). The addition of increasing amounts of cross-linking and bundling proteins to F-actin networks results in progression from a viscous solution to development of a gel with reduced deformability and increased rigidity. Filamin appears to be an essential cytoskeletal protein for determining the mechanical characteristics of cells (37). Cells that are deficient in filamin or in which its level of expression is reduced demonstrate unstable cell membranes, motility defects, and increased sensitivity to injury and death as a result of mechanical trauma (9, 10, 37). With increased membrane localization of filamin in response to stretch, cell membranes become stiffer (17). Mutations in  $\alpha$ -actinin-4, the predominant isoform in podocytes, result in glomerular sclerosis in humans and mice, demonstrating that abnormal function of cytoskeletal proteins is sufficient to cause glomerular disease (23).

The mechanical properties of podocytes should permit them to maintain their shape and structure, particularly the slit diaphragm, and the integrity of glomerular capillaries, in the presence of capillary hemodynamic forces. The foot processes that form the slit diaphragms and the secondary processes that give rise to them contain actin bundles and cross-linking and bundling proteins, including  $\alpha$ -actinin-4 and cortactin and presumably other less well-characterized proteins such as fil-

Address for reprint requests and other correspondence: R. T. Miller, Case Western Reserve Univ., Renal Section, Louis Stokes VAMC, 10701 East Blvd., Cleveland, OH 44106 (e-mail: rtm4@case.edu).

The costs of publication of this article were defrayed in part by the payment of page charges. The article must therefore be hereby marked "advertisement" in accordance with 18 U.S.C. Section 1734 solely to indicate this fact.

amin (12, 21). If forces on the capillary exceed a certain level, or if abnormalities of the cytoskeleton occur, the podocytes should not function normally and should undergo pathological responses such as foot process effacement and simplification, and ultimately detachment and cell death. The consequences could be initial dilation and ultimately rupture and collapse of the capillary.

To understand how cytoskeletal structure relates to the mechanical properties of podocytes, we compared actin and filamin expression in conditionally immortalized wild-type (WT) podocytes and podocytes derived from a mouse that expresses the HIV genome and that serves as a model for HIVAN and FSGS (5, 25). Filamin was studied because of its importance in cytoskeletal structure and because a previous representational difference analysis (RDA) of WT and HIVAN conditionally immortalized podocytes that resulted in identification of podocan, a protein that is expressed at high levels in HIVAN cells, also demonstrated that filamin A mRNA was reduced in HIVAN cells (32) (LA Bruggeman, unpublished results). The mechanical properties of the podocytes were measured using microaspiration and atomic force microscopy (AFM), both techniques that assess deformability or stiffness of cells. Cell stiffness or deformability is measured as force per unit area, and the unit is the Pascal (Pa), where one Pa is equal to 1 Newton/m<sup>2</sup>. We found significant differences in actin and filamin expression and distribution in these two cell types corresponding to a marked reduction in HIVAN podocyte cell stiffness. These differences indicate that the altered mechanical properties of HIVAN podocytes may contribute to the development of HIV nephropathy.

## METHODS

**Cell culture.** WT and HIV-1 transgenic (HIVAN) podocytes were maintained in RPMI 1640 with 10% FBS, 100 U/ml penicillin, 100 µg/ml streptomycin, 10 U/ml interferon-γ (IFN) at 33°C (permissive conditions) and 10% carbon dioxide. For differentiation, cells were plated on surfaces coated with type I collagen and grown without IFN at 37°C (nonpermissive conditions) for 10–14 days.

**Antibodies.** The anti-peptide filamin-A-specific antibody was produced using a synthetic peptide. The peptide, PLRSQQLAPQY, corresponding to AA 1751–1762 of the human filamin sequence that is identical in the mouse sequence (AA 1732–1742) and is localized in the first hinge region was synthesized and coupled to KLH at the University of Florida Protein core (Gainesville, FL). The conjugated peptide was injected into two rabbits and antibodies were produced by Cocalico Biologicals (Reamstown, PA). The antibodies from both rabbits recognize proteins of ~280 kDa in human, mouse, and dog cells but do not recognize a protein in the human melanoma cell line, M2, that lacks filamin. The anti-α-actinin (sc-15335), anti-actin (sc-8432), and anti-p125FAK (scs-557) antibodies were from Santa Cruz Biotechnology.

**Immunofluorescence.** At varying stages of differentiation, cells were fixed with cold acetone, permeabilized in 0.1% saponin, and stained with either an anti-filamin antibody (1:100), anti-synaptopodin antibody (1:10), or Texas Red-labeled phalloidin. Primary antibodies were counterstained with the appropriate secondary antibodies labeled with Oregon green or Texas red. Cells were then visualized using a Zeiss fluorescent microscope (model LSM-5 Pascal) and imaged by AxioVision Viewer 3.0.

**Cell fractionation.** WT and HIVAN podocytes were seeded onto collagen-coated 150-mm dishes and differentiated for a period of 10–14 days. Culture plates were ~80–90% confluent when harvested in cold HME buffer containing protease inhibitors and homogenized

with 50 strokes of a Dounce homogenizer. Cell nuclei were pelleted and the protein concentration of the postnuclear supernatant was determined using a BCA protein assay. Equivalent protein extracts were centrifuged at 15,000 rpm for 1 h at 4°C to separate particulate from soluble fractions. Crude membrane pellets were resuspended in equal volumes of sample buffer and boiled for 3–5 min.

**Western blotting.** Samples were subjected to 6% SDS-PAGE and after transfer to a nitrocellulose membrane, antibodies were stained with Ponceau S to confirm equal protein loading across lanes. Immunoblots were processed with primary antibody indicated and visualized using enhanced chemiluminescence. Band densitometry was performed using Scion Image software and analyzed for significance using Student's *t*-test.

**Microaspiration.** Cells were grown on rectangular glass coverslips (~9 × 9 mm) coated with type I collagen and differentiated. They were incubated with the fluorescent membrane dye, carbocyanide DiC<sub>18</sub> (Molecular Probes, Eugene, OR) for visualization, washed with PBS, and placed on a fluorescence microscope stage. Under direct visualization, the aspiration pipette (parallel to the microscope stage and the photomultiplier tube) was attached to the lateral aspect of the cell membrane. Aspiration was initiated with negative pressures of 1 mmHg, and the amount of membrane entering the pipette was tracked using a video camera. After a period of 3 min, the negative pressure was increased in increments of 1 mmHg until the membrane ruptured. The length of the process in the pipette was determined using the video images and normalized for the diameter of the pipette. Fluorescence images were acquired with a Zeiss Axiovert 100TV microscope (Zeiss, Jena, Germany) and a CCD camera (Micromax, Princeton Instruments, Trenton, NJ) via a ×40 Plan-Apochromat lens (numerical aperture 0.75). Pipettes were pulled from borosilicate glass capillaries (SG 10 glass, Richland Glass, Richland, NJ) and drawn to an internal diameter of ~2 µm and an external diameter of 4–5 µm. They were filled with 30% serum, placed in a microaspiration device (pneumatic transducer tester Biotek Inst, Winooski, VT), and then placed next to the cell membrane (6).

**AFM.** AFM imaging was performed with a Bioscope IIIa atomic force microscope (Digital Instruments, Santa Barbara, CA). The samples, cells grown on collagen-covered glass coverslips in a 35-mm plastic tissue culture dish, were attached to the probe chamber and imaged at room temperature. Imaging was performed in fluid tapping mode using a DNP-S oxide-sharpened silicon nitride probe (digital instruments) with a spring constant of 0.32 N/m at a scanning frequency of 5 Hz. Elasticity mapping was performed at 1 Hz and cell stiffness maps were generated using the Nanoscope IIIa software (version 5.12, Digital Instruments). WSxM freeware (version 3.0 Nanotec, Madrid, Spain) was used for height measurements and elasticity measurements. Elasticity values were calculated using the Hertz method (11).

## RESULTS

**Expression of filamin and synaptopodin in WT and HIVAN podocytes.** Based on the reduction in filamin mRNA in HIVAN cells, the importance of filamin in determining the mechanical characteristics of animal cells, and the possibility that HIVAN podocytes could have substantial structural differences compared with normal cells, we pursued analysis of filamin in these two cell types. As conditionally immortalized podocytes differentiate, their size and shape change, and they express proteins including synaptopodin characteristic of differentiated cells. Figure 1 shows WT podocytes over a 12-day course of differentiation stained for filamin, actin, and synaptopodin. In the undifferentiated state, the cells are polygonal, do not express synaptopodin, and express actin and filamin. Cortical F-actin is prominent, filamin is distributed throughout the

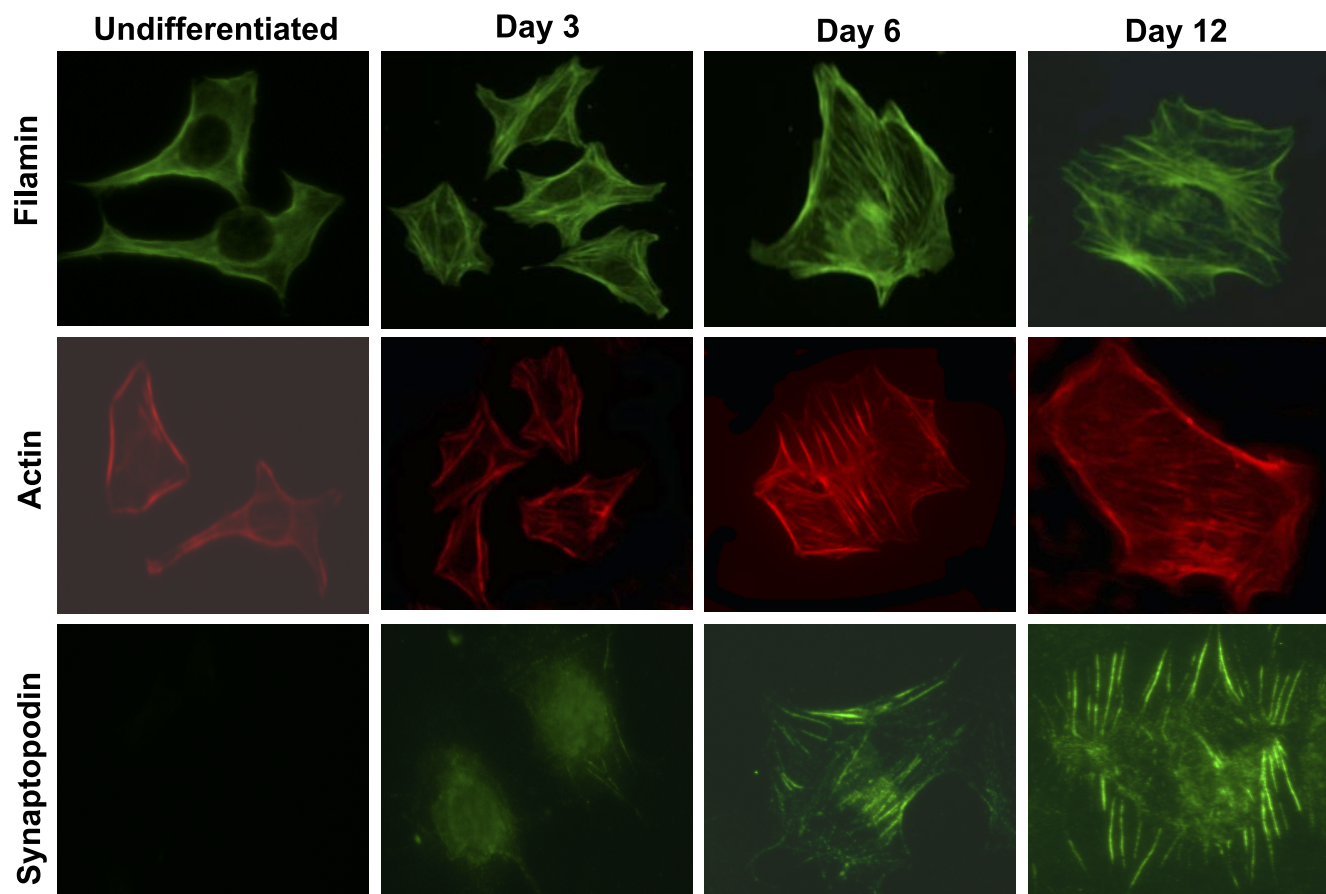


Fig. 1. Wild-type (WT) podocytes stained for filamin (*top*), actin (*middle*), and synaptopodin (*bottom*) at 4 different stages of differentiation. Cells demonstrate a progressive increase in size as well as the formation of prominent filamin, actin, and synaptopodin-containing fibers. The presence of synaptopodin fibers serves as a marker for podocyte differentiation. Cells were plated on collagen-coated coverslips and propagated at 37°C in the absence of IFN- $\gamma$  for the periods of time indicated. They were fixed in acetone and stained with the antibodies indicated. F-actin was stained with Texas red-labeled phalloidin. All images were obtained at  $\times 40$  magnification and the exposure times were the same for each individual antibody.

cytoplasm, and relatively few stress fibers are seen. As podocytes differentiate, they become larger and broader, synaptopodin is expressed, and stress fibers where all three proteins are present become prominent. Characterization of our rabbit polyclonal anti-filamin antibody is shown in Fig. 2. The antigen was a peptide derived from the first hinge region (AA 1751–1762) of the human sequence (18). Figure 2A shows Western blot peptide blocking experiments with whole cell extracts from WT and HIVAN podocytes. The specific peptide is the antigenic peptide, and the nonspecific peptide is derived from the COOH terminus of filamin. The specific antigenic peptide completely blocked the signal at 280 kDa representing filamin, but the nonspecific peptide had no effect. In similar studies, the antibody did not detect a band in M2 cells, a melanoma cell line that lacks filamin (9). Figure 2B shows that in immunofluorescence experiments, the specific peptide blocks the signal demonstrating that the antibody is specific both for Western blotting and immunofluorescence. As suggested in Fig. 1, differentiation of WT podocytes results in increased filamin expression. The level of filamin expression in whole cell extracts of undifferentiated and differentiated WT and HIVAN podocytes was compared using Western blotting. Figure 3A shows representative immunoblots comparing expression of filamin, p125FAK, and actin from WT-undifferentiated,

HIVAN-undifferentiated, WT-differentiated, and HIVAN-differentiated podocytes. Sample loading for the blots was normalized for protein content of the samples and also blotted for p125FAK as an additional control. We found that the level of p125FAK expression does not vary among these cell types but that the content of cytoskeletal proteins such as filamin is variable. Figure 3B shows summary data from scanning four blots. Filamin content is increased,  $\sim 1.5$ -fold in the differentiated WT podocytes over the other cell types, where its level of expression is similar. The level of expression of p125FAK and actin is similar in all cell types. Figure 4, *top*, shows immunofluorescence images of undifferentiated and differentiated WT and HIVAN podocytes stained for filamin and synaptopodin. Only in the WT-differentiated podocytes is a significant level of synaptopodin seen. These cells are broad, flat, and contain regions of filamin concentration at their edges consistent with a subcortical membrane pattern of expression as well as in stress fibers. Synaptopodin is centrally loaded and appears to be associated with stress fibers. The other cells (undifferentiated WT and undifferentiated and differentiated HIVAN cells) remain relatively small, express filamin, and have minimal expression of synaptopodin. In Fig. 4, *E* and *F*, the crude membrane fraction of undifferentiated and differentiated WT and undifferentiated and differentiated HIVAN

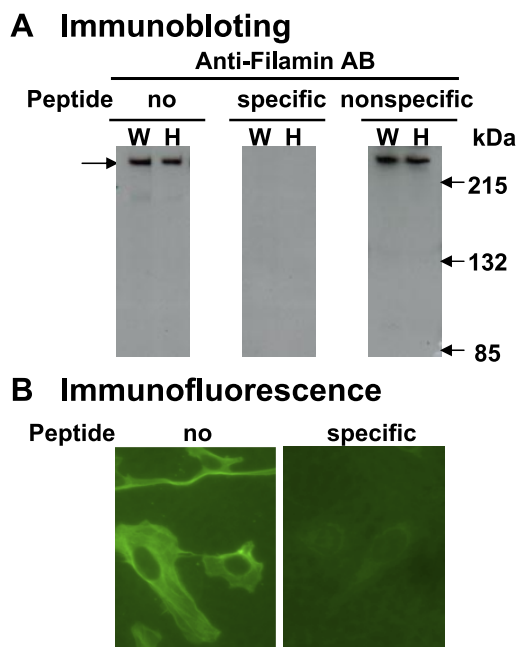
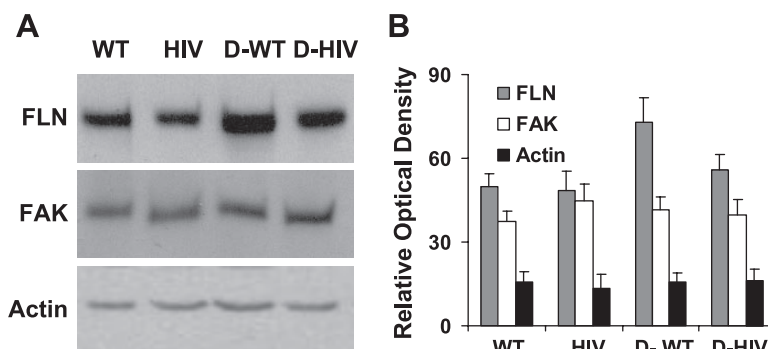


Fig. 2. Characterization of the anti-filamin antibody. *A*: identical panels with whole cell lysates from WT (W) and HIVAN (H) podocytes blotted with the anti-filamin antibody (*left*), the anti-filamin antibody incubated with the antigenic peptide (*middle*), and a peptide derived from the COOH terminus of filamin (*right*). *B*: immunofluorescent images of undifferentiated podocytes incubated with the anti-filamin antibody without peptide (*left*) and the anti-filamin antibody preincubated with the antigenic peptide (*right*). Magnification  $\times 40$ .

podocytes was used for Western blotting for filamin. Figure 4E is a representative Western blot, and Fig. 4F shows summary data from five separate experiments. In the differentiated WT cells, filamin expression is increased  $\sim 1.7$ -fold over the level in the other cell types. This fold increase is greater than that found in whole cell extracts (Fig. 3) because the membrane fraction appears to be enriched in filamin. HIVAN podocytes fail to differentiate fully. They remain small and polygonal, and even with removal of IFN, plating on collagen, and growth at  $37^{\circ}\text{C}$ , continue to proliferate (4). Additionally, as shown in Fig. 4D, their pattern of filamin expression after 12 days of differentiation appears similar to that of undifferentiated cells and they express substantially less synaptopodin than differentiated WT cells. As shown in Figs. 3 and 4, with differentiation the level of filamin expression in HIVAN podocytes increases minimally if at all and appears similar to that of undifferentiated WT cells.

Fig. 3. Expression of filamin in WT and HIVAN podocytes. Whole cell extracts from undifferentiated WT, undifferentiated HIVAN (HIV), differentiated WT (D-WT), and differentiated HIVAN (D-HIV) podocytes were prepared, normalized for total protein, and blotted with antibodies to filamin, p125FAK, and actin using the same membrane. *A*: representative blots for filamin (FLN), p125FAK (FAK), and actin. Four blots were scanned and the density of the bands for each of the proteins was quantitated using Scion Image software. *B*: summary data from 4 similar blots  $\pm$  SD. Filamin expression in D-WD was different from the D-HIV, WT, and HIV samples ( $P = 0.03$  by Student's *t*-test for comparison of means).



*Filamin:actin and actinin:actin ratios in WT and HIVAN podocytes.* Filamin affects the mechanical properties of the cytoskeleton through its ability to cross-link filamentous actin. The degree of actin cross-linking by filamin and other actin cross-linking proteins such as  $\alpha$ -actinin can be inferred by measuring the ratios of cross-linking proteins to actin. We measured filamin:actin and actinin:actin ratios in whole cell extracts from undifferentiated and differentiated WT and HIVAN podocytes using Western blotting and estimating the protein:protein ratio from the relative densities of the band in the immunoblots. As shown in Fig. 5, the level of filamin expression is increased in differentiated podocytes compared with WT undifferentiated and HIVAN cells. The level of  $\alpha$ -actinin expression is maximal in differentiated WT podocytes but also increased in differentiated HIVAN podocytes compared with undifferentiated podocytes. The levels of actin expression are similar in undifferentiated cells (WT and HIVAN) and increased in differentiated cells. The consequence of the increase in filamin expression with differentiation of the WT podocytes is that their filamin:actin ratio is 1.5, while that of the other cells is  $\sim 1$  (Fig. 5, *middle*). The actinin:actin ratio is  $\sim 0.9$  for the WT podocytes and 0.6 for the HIVAN podocytes but is not altered by the state of differentiation (Fig. 5, *bottom*). These results suggest that in the differentiated WT podocytes, actin may be more highly cross-linked by filamin, so that the cytoskeletons of the WT and HIVAN cells could have different mechanical properties (37, 39, 40).

*Measurement of membrane characteristics by microaspiration.* The membrane elasticity of differentiated WT and HIVAN podocytes was analyzed using microaspiration. A pipette with an internal diameter of  $\sim 2 \mu\text{m}$  and an external diameter of  $4\text{--}5 \mu\text{m}$  was attached to a single cell that had been loaded with the fluorescent membrane dye, DiC<sub>18</sub>. The pipette and cell membrane were visualized with a fluorescence microscope and CCD camera. When a seal was achieved, negative pressure was applied, and the membrane was drawn into the pipette. If the cell ruptured, the membrane was not visible in the pipette, but if the membrane remained intact, the negative pressure was increased, and the progress of the membrane in the pipette followed. Figure 6 shows typical images from microaspiration studies with WT (*A*) and HIVAN (*B*) podocytes just before rupture of the membrane. The column of membrane drawn into the pipette is considerably longer in the WT than the HIVAN cells and corresponds to increased elastic deformability of the WT cells. Figure 6C shows traces representing the length of membrane processes from microaspira-

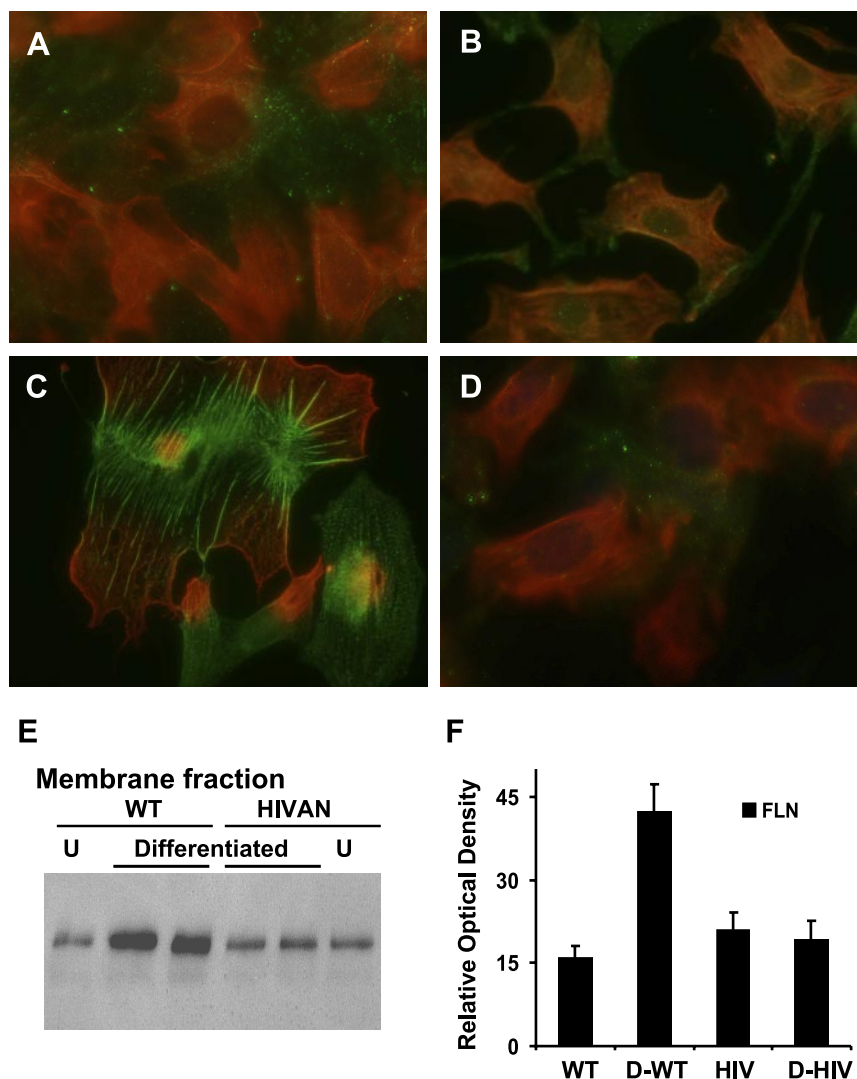


Fig. 4. Expression and distribution of filamin and synaptopodin in WT and HIVAN podocytes. *Top*: immunofluorescence of undifferentiated WT podocytes (A), undifferentiated HIVAN podocytes (B), differentiated WT podocytes (C), and differentiated HIVAN podocytes (D) stained for filamin (red) and synaptopodin (green). Differentiated cells were plated on collagen-coated coverslips and grown for 12 days at 37°C in the absence of IFN- $\gamma$ , and undifferentiated cells were plated on glass coverslips and grown for 12 days at 32°C in the presence of IFN- $\gamma$ . The cells were fixed in acetone and stained with the antibodies indicated. All images were obtained at  $\times 40$  magnification. *E*: representative Western blot for filamin from membrane fraction of WT and HIVAN podocytes [undifferentiated (U)]. Duplicate samples from differentiated WT and HIVAN membranes and single samples from undifferentiated WT and HIVAN are shown. *F*: summary densitometry data from 5 separate Western blots from WT and HIVAN podocytes. The difference between the means of the D-WT and D-HIVAN membranes was significant ( $P = 0.0002$  by Student's *t*-test for comparison of means).

tion studies as a function of time at four different pressures. The traces end when the cells rupture. Most of the HIVAN cells rupture at low negative pressures, while the WT cells persist to negative pressures up to  $-8$  mmHg. Additionally, the processes for the WT cells were longer than those for the HIVAN podocytes. Figure 7 shows the number of WT or HIVAN podocytes that ruptured at different pressures. Most of the HIVAN cells ( $n = 7$ ) ruptured at 1 mmHg of negative pressure, and all ruptured when 4 mmHg negative pressure was achieved. Although some WT cells ruptured at low pressures, one-third of them required 8 mm of Hg to rupture, a pressure fourfold greater than that tolerated by the HIVAN podocytes. These results demonstrate that the membranes of the HIVAN cells are more fragile than the WT cells which have greater distensibility.

*Measurement of membrane characteristics by atomic force microscopy.* We used AFM to perform surface scans and force-displacement measurements of the podocytes. The surface scan of the WT podocytes was performed at 5 Hz and shows that they are broad, flat cells with prominent fibers visible beneath the cell membrane. The broad flat area constituting the majority of the cell is  $\sim 1.5$ - $\mu\text{m}$  thick. The

HIVAN cells could not be scanned in this mode because they were ruptured by the probe, but they are thicker than the WT cells, on the order of 4 to 6  $\mu\text{m}$ . The force-displacement analysis demonstrates that the HIVAN cells are much softer than the WT cells. The stiffness calculations were based on only the first 100 nm of indentation to avoid the confounding factor of substrate characteristics. Figure 8A shows a comparison of the stiffness of WT ( $17.2 \pm 2.66$  kPa) and HIVAN cells ( $4.2 \pm 0.42$  kPa). For these studies, WT ( $n = 10$ ) and HIVAN ( $n = 13$ ) cells were studied with two to three measurements of each cell. Figure 8B shows representative force-volume curves for WT and HIVAN podocyte using AFM. The curves represent deflection of the AFM probe as a function of force applied. The curve for the WT cells is much steeper indicating greater deflection of the probe (less deformation of the cell) and a very stiff cell, while the curve for the HIVAN cells is more shallow with less deflection of the probe (more deformation of the cell with the same force), indicative of a significantly softer cell. Figure 8C shows a surface stiffness map of a representative WT and HIVAN cell. For these images, curves from each color area of the whole cell stiffness map were ana-

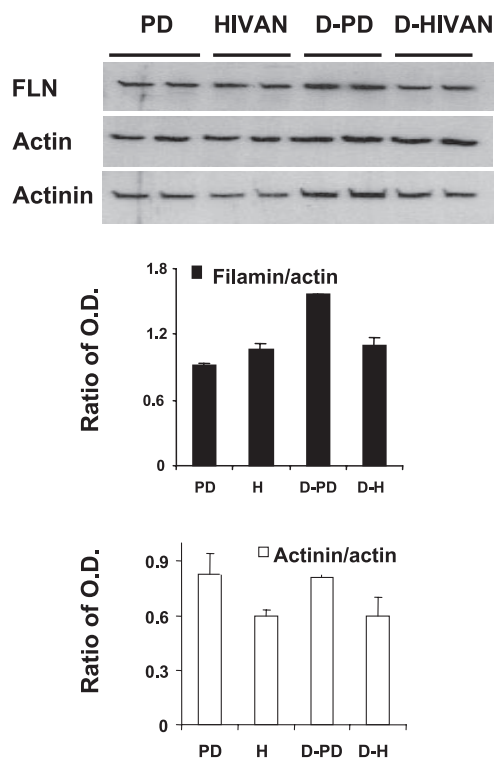


Fig. 5. Filamin:actin and actinin:actin ratios in WT and HIVAN podocytes. Filamin, actin, and  $\alpha$ -actinin levels were compared in whole cell lysates from undifferentiated and differentiated WT and HIVAN podocytes. Duplicate samples were prepared and equal amounts of protein were loaded in each lane. The same membranes were blotted separately for filamin, actin, and  $\alpha$ -actinin. The figure shown is representative of 3 separate blots. The bands were scanned separately and quantified using the NIH Scion Image program. The ratios were calculated based on the density of the bands with actin as the denominator.

lyzed and stiffness values were calculated. Colors were assigned to a range of stiffness values and then superimposed on the cell image. The region above the nucleus of the WT cells is relatively soft, 2.5–3.5 kPa, while the remainder of the cell, the wide flat region surrounding the nucleus, is considerably stiffer with the yellow areas 7.8–15.2 kPa, and the green areas 16.9–23.9 kPa. The softness of the nuclear region may explain some of the measurements of soft regions in the WT cells. The stiffest regions of these cells are at the edge where they are on the order of 1- to 1.5- $\mu$ m thick. In contrast, the central region of the HIVAN cells (yellow) is relatively stiff (5.7–9.1 kPa) and the peripheral region including the edges that are 1  $\mu$ m or less thick are softer (2.7–5.9 kPa). This observation is at variance with the concept that the edges of cells are usually thin with a dense, stiff actin network, and represents another clear difference between the WT and HIVAN podocytes.

## DISCUSSION

The composition and structure of the cytoskeletons of WT and HIVAN podocytes differ with less filamin expression and more restricted distribution in the HIVAN cells. This difference in cytoskeleton composition and structure corresponds to markedly different biophysical properties of the two cell types. The WT cells are significantly less deformable than the HIVAN podocytes. These differences in structural and bio-

physical characteristics if also present in vivo could contribute to the loss of glomerular capillary structure found in collapsing glomerulonephritis associated with HIV infection.

The two techniques that were used to measure the mechanical properties of the cells, microaspiration and AFM, measure different aspects of cell deformability. Microaspiration is not intended as a model for injury, but as an assay for the mechanical properties of the cell membrane. Microaspiration measures membrane deformations on the order of microns that occur over relatively large areas of the cell surface over time scales of tens to hundreds of seconds. These deformations involve both passive viscoelasticity and active remodeling of the cell structure. In contrast, AFM measures deformations on a subsecond time scale with indentations on the order of 100 nm at the surface of structures at least 1.5- $\mu$ m thick, corresponding to smaller strains that are more likely to reflect local elasticity than active remodeling. The elasticity of the cell surface can be affected by the elastic characteristics of the cytoskeleton, the attachment of the cell membrane to the cytoskeleton, and the physical characteristics of the cell membrane. The consistent finding by both methods of large mechanical differences between WT and HIVAN podocytes supports the hypothesis that a weakened actin cytoskeleton can lead to less elastic resistance and higher probability of cellular damage by stresses imposed within the glomerulus in cells lacking normal filamin levels.

The mechanical properties of the WT podocytes are unusual in that in the majority of these cells, the area surrounding the nucleus, is extremely stiff, on the order of 20 kPa. This region is flat, 1- to 1.5- $\mu$ m thick, with conspicuous cytoskeletal fibers and presumably little cytoplasm, characteristics that may be similar to podocyte primary processes and foot processes. Some other cell types that are also flat such as endothelial cells can have stiffness values as high as 20 kPa, but other endothelial cells are softer with stiffness values on the order of 10 kPa, and some microvascular cells are very soft with stiffness values as low as 1–5 kPa. Fibroblasts grown on glass coverslips have stiffness values on the order of 5–12 kPa (34) (I Levental and PA Janmey, unpublished observations). The average value of 17 kPa for the WT, differentiated podocytes includes several measurements in the soft nuclear region where the stiffness was on the order of 2.5–3.5 kPa, while the remainder of the cell, the flat thin region that contains multiple stress fibers, was greater than 7.8 kPa, and as high as 23.9 kPa. We believe that values on the order of 20 kPa are an accurate estimate of the stiffness of these cells and that it is independent of the properties of the substrate because our calculations of stiffness used only the first 100 nm of indentation. Consequently, the stiffness values reported for the WT, differentiated podocytes are conservative and could in fact be higher.

The HIVAN cells are much softer than their WT counterparts and contain substantially less filamin. These cells are comparable to fibroblasts in terms of stiffness and size. An interesting feature of these cells is that their edges are softer than their centers. In most cells plated on plastic, the edges contain actin- and filamin-rich structures that are stiffer than the remainder of the cell (34). This characteristic appears to be unusual and may reflect a property of HIVAN podocytes that

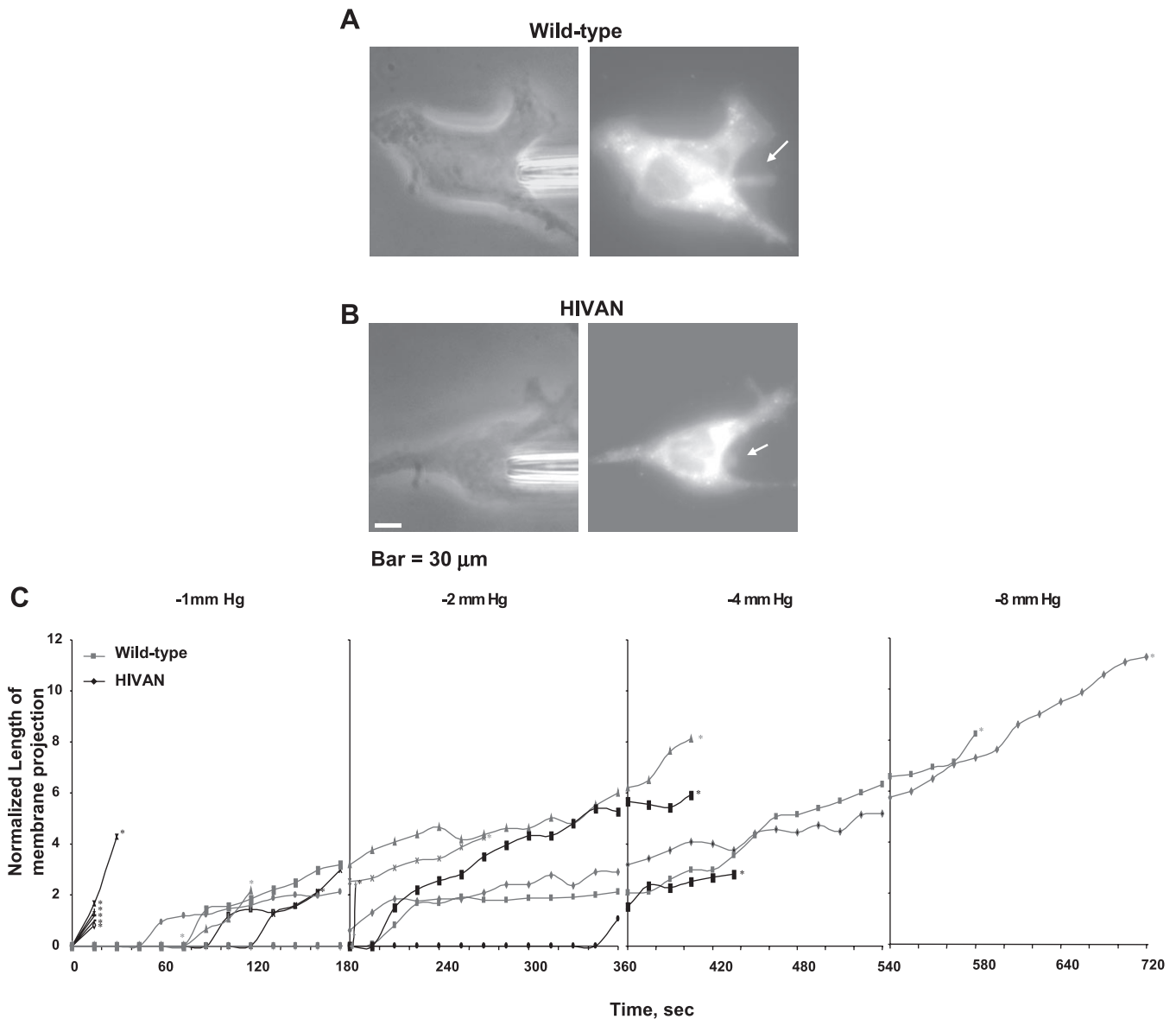


Fig. 6. Microaspiration of WT and HIVAN podocytes. *Top*: microaspiration of a WT cell (A) with attachment of the pipette under phase contrast microscopy (*left*) and aspirating a column of membrane under fluorescence (*right*). *B*: HIVAN podocyte under phase contrast (*left*) and aspiration of membrane immediately before rupture at  $-1$  mmHg. Differentiated cells on collagen-coated coverslips were incubated with the membrane fluorescent dye Di-C18, washed, and visualized under a phase contrast microscope for placement of the micropipette. At the beginning of the experiments, negative pressure was applied to the pipette, and the distance the column of membrane moved up the pipette was recorded with a digital camera. *C*: plot of normalized length of membrane projection for WT (pink) and HIVAN (blue) cells (*x*-axis) and time on the *y*-axis. The negative pressure steps are shown at the *top*.

contributes directly to HIV nephropathy. The characteristics of these cells may be attributable to many factors in addition to their reduced levels of filamin. They contain the HIV genome and appear to have a generalized defect in differentiation that includes increased levels of proliferation markers, NF- $\kappa$ B activity, an increased rate of apoptosis, increased desmin expression, loss of contact inhibition, reduced expression of synaptopodin, WT-1 and filamin associated with an altered cytoskeleton (2, 5, 25, 33, 35). The HIV nef and tat genes may be of particular importance in these processes (7, 20, 38). Nevertheless, altered filamin expression levels and distribution are likely to be important determinants of the physical characteristics of cells, and alterations in other proteins that could explain these differences have not been reported.

Filamin has three essential cell functions, cross-linking actin, mediating actin-membrane connections, and serving as a scaffold for numerous cellular and transmembrane proteins (15, 37). Three filamin genes have been identified, FLNa, a ubiquitously expressed form, FLNb which is also widely expressed, but less abundant than FLNa, and FLNc which is primarily expressed in muscle. Although associated with the cortical actin cytoskeleton, filamin is also present in significant amounts in the soluble fraction of cells (31, 37). Filamin has not been studied in podocytes, but it is localized with F-actin in the cytoskeleton as shown above, consistent with its localization in other cell types (37). Filamin exists as a homodimer with the dimerization domain at the COOH terminus. Each filamin monomer has an approximate MW of 280 kDa with an

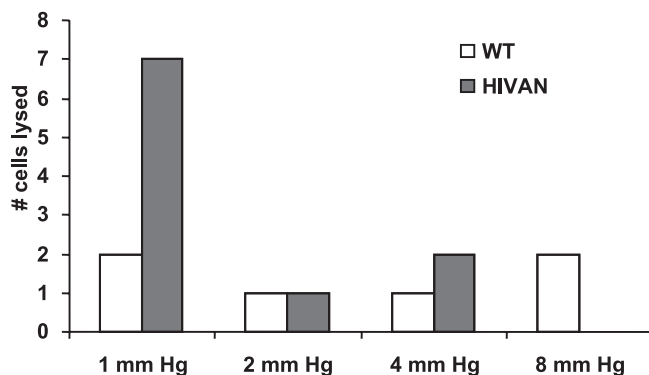


Fig. 7. Frequency of cell rupture with microaspiration. Single WT and HIVAN podocytes were analyzed using microaspiration. The pipette was attached to the lateral cell membrane, and negative pressure was applied initially at 1 mmHg, and progressing up to 8 mmHg in steps as shown over several minutes. Six WT and 10 HIVAN cells were analyzed. The graph shows the number of cells that ruptured at a given negative pressure on the y-axis and the negative pressure on the x-axis.

NH<sub>2</sub>-terminal actin binding domain composed of two calponin homology domains, 24 IgG-like 96 AA repeats that form stiff, rod-like structures, two hinge regions between repeats 15 and 16, and 23 and 24, and a dimerization domain in repeat 24. These structural features give the homodimer the characteristics of a leaf-spring in contrast to other actin-binding proteins that behave as short rigid rods (37). The dimerization of filamin coupled with its hinge domains give it and the actin networks its cross-links unique mechanical properties that are more elastic than those conferred by other actin bundling and cross-linking proteins.

The actin cross-linking function of filamin has been studied in cells and in vitro with purified proteins. Filamin cross-links actin in a perpendicular mesh in the subcortical region of cells and this cross-linking function of filamin is believed to be the principal determinant of the mechanical characteristics of cells (37). Cells and actin-filamin solutions have the characteristic that they accommodate small forces and resist larger applied forces by a strain-dependent stiffening of the matrix (14, 15, 36). In purified gels, the greater the amount of filamin, the stiffer the matrix. This relationship is nonlinear such that if the concentration of filamin doubles, the stiffness more than doubles. Actin-filamin networks behave more like covalently linked gels than viscous solutions at filamin:actin ratios > 1:200 (8, 15, 39). Solutions (gels) with filamin:actin ratios on the order of 1:150–1:740 are characterized by stiff but elastic cross-linked f-actin networks with X, Y, or T junctions of actin fibers. The stiffness of the network results from the ability of filamin to form fiber junctions at angles approaching 90°, and the elasticity of the networks results from the hinged spring-like characteristics of filamin and the entropic elasticity of the actin filaments between crosslinks. Filamin:actin ratios of 1:10–50 result in actin bundling and the formation of fibers with elasticity due to filamin's structure (37, 39, 40). This information means that alterations in the level of filamin expression will clearly affect the mechanical properties of actin-filamin networks.

The effects of filamin on the mechanical characteristics of cells have been studied to a limited degree. In intact cells, actin and filamin concentrations and ratios are nonuniform, and

additional cytoskeletal proteins are present. In nonmuscle cells, the filamin:actin ratio is believed to be on the order of 1:50–1:100, presumably with regions of significantly higher and lower ratios (14). M2 melanoma cells that lack filamin have unstable membranes, significantly reduced motility, a reduced elastic modulus, and are more susceptible to injury and apoptosis in response to mechanical force than the A7 cells (9, 16). In the M2 cells, the amount of other actin-associated proteins ( $\alpha$ -actinin, fodrin, gelsolin, and profilin) is unchanged compared with control filamin-replete A7 melanoma cells, so the altered characteristics of the M2 cells are attributable to the absence of filamin (9). When the level of filamin expression or activity is reduced using siRNA or interfering filamin constructs fibroblasts become increasingly sensitive to mechanical injury (22). Consequently, the reduced level of filamin expression in HIVAN cells could have a number of adverse effects including making them more susceptible to mechanical injury, possibly reducing motility, and leading to reduced resistance to deformation.

Mutations in  $\alpha$ -actinin-4, the predominant  $\alpha$ -actinin isoform expressed in podocytes, that increase the affinity of  $\alpha$ -actinin-4 for actin result in a familial form of focal glomerular sclerosis (23). Alterations in the behavior of  $\alpha$ -actinin-4 would be expected to affect cell behavior and structure because of its effects on actin and its interactions with cytoskeletal and transmembrane proteins (30). The half-life of the protein is reduced, it appears to aggregate in cultured podocytes, and is less dynamic than the WT protein (41). The mechanical properties of cells expressing mutant forms of  $\alpha$ -actinin-4 have not been reported, but clearly actin binding proteins are important for podocyte function because mutations result in a phenotype similar to that found with other podocyte proteins such as nephrin, podocin, and CD2AP (24).

In glomerular podocytes, actin is found in the foot processes and primary processes in the form of thick filaments associated with  $\alpha$ -actinin, cactactin, and synaptopodin and presumably other proteins such as filamin (12, 21). The cytoskeleton of podocytes has not been fully defined, but presumably it also has an actin network beneath the plasma membrane in the primary and foot processes where actin, filamin,  $\alpha$ -actinin, and other cytoskeletal proteins interact resulting in the unique physical characteristics of these cells. The functions and distributions of these actin cross-linking proteins overlap indicating that they probably have complementary functions so that the loss of any one of them would result in specific defects that would result in disease. The HIVAN podocytes have reduced expression of filamin and synaptopodin. Despite the role of synaptopodin in regulating the actin bundling activity of  $\alpha$ -actinin-4, the structural consequences of synaptopodin loss are not dramatic, showing no obvious abnormality under basal conditions and requiring an insult to be manifest (1). Consequently, loss of synaptopodin may contribute to, but not explain completely, the markedly abnormal structural and mechanical characteristics of the HIVAN podocytes. Of the actin-associated proteins that contribute to the physical characteristics of cells, loss of filamin or its abnormal distribution or function should have the most dramatic effect based on studies in vitro and in cultured cells (37).

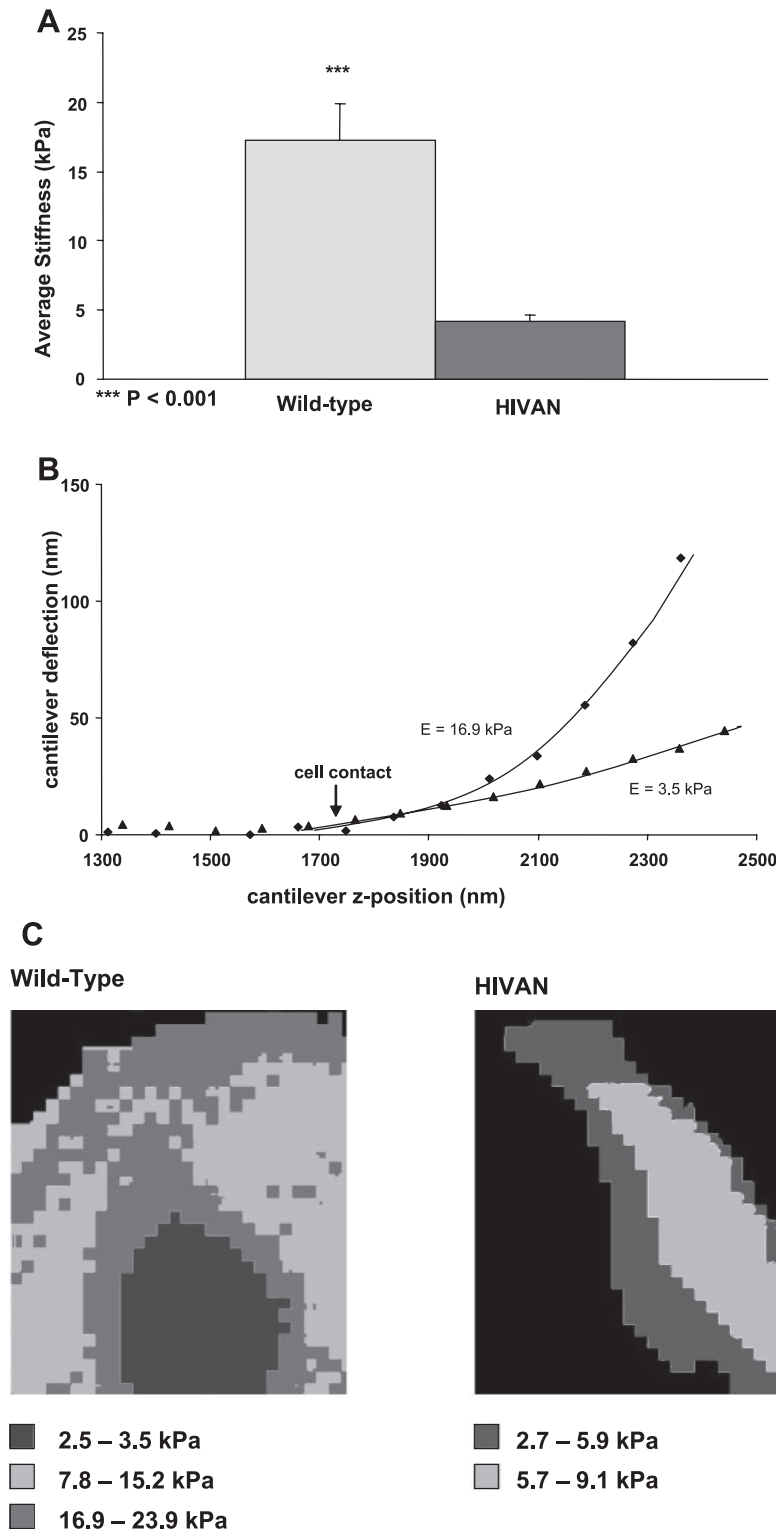


Fig. 8. Force-volume analysis for WT and HIVAN podocytes using AFM. *A*: comparison of the stiffness measurements of WT and HIVAN podocytes. Two or 3 force-displacement measurements were made at random points on 10 WT and 13 HIVAN cells. The first 100 nm of the indentation was used for calculations to minimize the effect of the substrate (glass). *B*: representative force-displacement curves for each of the cell types (WT blue diamonds and steep curve, HIVAN red triangles and shallow curve). The curves represent deflection of the AFM probe as a function of force applied. The values *E*, or elasticity, are calculated from the curve and are shown as 16.9 kPa for WT and 3.5 kPa for the HIVAN cells. *C*: surface stiffness map of WT and HIVAN podocytes. For these images, multiple stiffness values were calculated for each cell, and the positions were recorded. Colors were assigned to a range of stiffness values and then superimposed on the cell images. For the WT cells, blue corresponds to values ranging from 2.5 to 3.5 kPa, yellow corresponds to areas ranging from 7.8 to 15.2 kPa, and green corresponds to areas ranging from 16.9 to 23.9 kPa. For the HIVAN cells, blue corresponds to regions ranging from 2.7 to 6.9 kPa, and yellow corresponds to areas ranging from 5.7 to 9.1 kPa.

The reduced filamin and synaptopodin levels we report here are likely not the only cytoskeletal defects in the HIVAN podocytes. Nevertheless, given the importance of filamin in the structure and integrity of the cytoskeleton, it is reasonable to conclude that the reduced levels of filamin found in these studies are related to the remarkable softness of the HIVAN podocytes compared with the WT cells. The

HIVAN podocytes would have a significantly reduced ability to support glomerular capillaries and might be less able to migrate or adjust to changes in capillary shape. In the presence of normal or increased hemodynamic forces, the capillary supported by a HIVAN podocyte could either dilate or collapse, both scenarios resulting in glomerulosclerosis (26).

## GRANTS

This work was supported by grants from the American Heart Association to C. Huang and R. T. Miller, National Institutes of Health (NIH) Grants DK-59985 and HL-41618, a VA Merit Review to R. T. Miller, NIH Grant GM-56218 to P. A. Janney, and the Leonard Rosenberg Research Foundation.

## REFERENCES

- Asanuma K, Kim K, Oh J, Giardino L, Chabanis S, Faul C, Reiser J, Mundel P. Synaptopodin regulates the actin-bundling activity of  $\alpha$ -actinin in an isoform-specific manner. *J Clin Invest* 115: 1188–1198, 2005.
- Barisoni L, Bruggeman LA, Mundel P, D'Agati VD, Klotman PE. HIV-1 induces renal epithelial dedifferentiation in a transgenic model of HIV-associate nephropathy. *Kidney Int* 58: 173–181, 2000.
- Barisoni L, Kriz W, Mundel P, D'Agati V. The dysregulated podocyte phenotype: a novel concept in the pathogenesis of collapsing idiopathic focal segmental glomerulosclerosis and HIV-associated nephropathy. *J Am Soc Nephrol* 10: 51–61, 1999.
- Barisoni L, Mokrzycki M, Sablay L, Nagata M, Yamase H, Mundel P. Podocyte cell cycle regulation and proliferation in collapsing glomerulonephritis. *Kidney Int* 58: 137–143, 2000.
- Bruggeman LA, Dikman S, Meng C, Quaggin SE, Coffman TM, Klotman PE. Nephropathy in human immunodeficiency virus-1 transgenic mice is due to renal transgene expression. *J Clin Invest* 100: 84–92, 1997.
- Byfield FJ, Aranda-Espinoza H, Romanenko VG, Rothblat GH, Levitan I. Cholesterol depletion increases membrane stiffness of aortic endothelial cells. *Biophys J* 87: 3336–3343, 2004.
- Conaldi PG, Botelli A, Baj A, Serra C, Fiore L, Federico G, Busolati B, Camussi G. Human immunodeficiency virus-1 Tat induces hyperproliferation and dysregulation of renal glomerular epithelial cells. *Am J Pathol* 161: 53–61, 2002.
- Coughlin MF, Puig-de-Morales M, Bursac P, Mellema M, Millet E, Fredberg JJ. Filamin A and rheological properties of cultured melanoma cells. *Biophys J* 90: 2199–2205, 2006.
- Cunningham CC, Gorlin JB, Kwiatkowski DJ, Hartwig JH, Janney PA, Byers R, Stossel TP. Actin-binding protein requirement for cortical stability and efficient locomotion. *Science* 255: 325–327, 1992.
- D'Addario M, Arora PD, Fan J, Ganss B, Ellen RP, McCulloch CAG. Cytoprotection against mechanical forces delivered through  $\beta_1$  integrins requires induction of filamin A. *J Biol Chem* 276: 31969–31977, 2001.
- Domke J, Radmacher M. Measuring the elastic properties of thin polymer films with the atomic force microscope. *Langmuir* 14: 3320–3325, 1998.
- Drenckhahn D, Franke RP. Ultrastructural organization of contractile and cytoskeletal proteins in glomerular podocytes of chicken, rat, and man. *Lab Invest* 59: 673–682, 1988.
- Flanagan LA, Chou J, Hevré F, Neujahr R, Hartwig JH, Stossel TP. Filamin A, the Arp2/3 complex, and the morphology and function of cortical actin filaments in human melanoma cells. *J Cell Biol* 155: 511–517, 2001.
- Gardel ML, Nakamura F, Hartwig J, Crocker JC, Stossel TP, Weitz DA. Stress-dependent elasticity of composite actin networks as a model for cell behavior. *Phys Rev Lett* 96: 088102, 2006.
- Gardel ML, Nakamura F, Hartwig JH, Crocker JC, Stossel TP, Weitz DA. Prestressed F-actin networks cross-linked by hinged filamins replicate mechanical properties of cells. *Proc Natl Acad Sci USA* 103: 1762–1767, 2006.
- Glogauer M, Arora P, Chou D, Janney PA, Downey GP, McCulloch CAG. The role of actin-binding protein 280 in integrin-dependent mechanoprotection. *J Biol Chem* 273: 1689–1698, 1998.
- Glogauer M, Arora P, Yao G, Sokolov I, Ferrier J, McCullough CAG. Calcium ions and tyrosine phosphorylation interact coordinately with actin to regulate cytoprotective responses to stretching. *J Cell Sci* 110: 11–21, 1997.
- Gorlin JB, Yamin R, Egan S, Stewart M, Stossel TP, Kwiatkowski DJ, Hartwig JH. Human endothelial actin-binding protein (ABP-280, non-muscle filamin): a molecular leaf spring. *J Cell Biol* 111: 1105, 1990.
- Hostetter TH, Olson JL, Rennke HG, Venkatachalam MA, Brenner BM. Hyperfiltration in remnant nephrons: a potentially adverse response to renal ablation. *Am J Physiol Renal Physiol* 241: F85–F93, 1981.
- Husain M, Gusella GL, Klotman ME, Gelman IH, Ross MD, Schwartz EJ, Cara A, Klotman PE. HIV-1 nef induces proliferation and anchorage-independent growth in podocytes. *J Am Soc Nephrol* 13: 1806–1815, 2002.
- Ichimura K, Kurihara H, Sakai T. Actin filament organization of foot processes in rat podocytes. *J Histochem Cytochem* 51: 1589–1600, 2003.
- Kainulainen T, Pender A, D'Addario M, Glogauer M, Lekic P, McCulloch CA. Cell death and mechanoprotection by filamin A in connective tissues after challenge by applied tensile forces. *J Biol Chem* 277: 21998–22009, 2002.
- Kaplan JM, Kim SH, North KN, Rennke H, Correia LA, Tong HQ, Mathis BJ, Rodriguiz-Perez JC, Allen PG, Beggs AH, Pollak MR. Mutations in ACTN4, encoding  $\alpha$ -actinin-4, cause familial focal segmental glomerulosclerosis. *Nat Genet* 24: 251–256, 2001.
- Kerjaschki D. Caught flat-footed: podocyte damage and the molecular bases of focal sclerosis. *J Clin Invest* 108: 1583–1587, 2001.
- Kopp JB, Klotman ME, Adler SH, Bruggeman LA, Dickie P, Marinov NJ, Eckhaus M, Bryant JL, Notkins AL, Klotman PE. Progressive glomerulosclerosis and enhanced renal accumulation of basement membrane components in mice transgenic for human immunodeficiency virus type 1 genes. *Proc Natl Acad Sci USA* 89: 1577–1581, 1992.
- Kriz W. Podocyte is the major culprit accounting for the progression of chronic renal disease. *Microsc Res Tech* 57: 189–195, 2002.
- Nagata M, Kriz W. Glomerular damage after uninephrectomy in young rats. II. Mechanical stress on podocytes as a pathway to sclerosis. *Kidney Int* 42: 148–160, 1992.
- Nagata M, Scharer K, Kriz W. Glomerular damage after uninephrectomy in young rats. I. Hypertrophy and distortion of capillary architecture. *Kidney Int* 42: 136–147, 1992.
- Nakamura F, Osborn E, Janney PA, Stossel TP. Comparison of filamin A-induced cross-linking and Arp2/3 complex-mediated branching on the mechanics of actin filaments. *J Biol Chem* 277: 9148–9154, 2002.
- Otery CA, Carpen O.  $\alpha$ -Actinin revisited: a fresh look at an old player. *Cell Motil Cytoskeleton* 58: 104–111, 2004.
- Ramsby ML, Makowski GS. Differential detergent fractionation of eukaryotic cells. *Methods Mol Biol* 112: 53–66, 1999.
- Ross MD, Bruggeman LA, Hanss B, Sunamoto M, Marras D, Klotman ME, Klotman PE. Podocan, a novel small leucine-rich repeat protein expressed in the sclerotic glomerular lesion of experimental HIV-associated nephropathy. *J Biol Chem* 278: 33248–33255, 2003.
- Ross MJ, Martinka S, D'Agati VD, Bruggeman LA. NF- $\kappa$ B regulates Fas-mediated apoptosis in HIV-associated nephropathy. *J Am Soc Nephrol* 16: 2403–2411, 2005.
- Rotsch C, Jacobsen K, Radmacher M. Dimensional and mechanical dynamics of active and stable edges in motile fibroblasts investigated by using atomic force microscopy. *Proc Natl Acad Sci USA* 96: 921–926, 1999.
- Schwartz EJ, Cara A, Snoeck H, Ross MD, Sunamoto M, Reiser J, Mundel P, Klotman PE. Human immunodeficiency virus-1 induces loss of contact inhibition in podocytes. *J Am Soc Nephrol* 12: 1677–1684, 2001.
- Storm C, Pastore JJ, MacKintosh FC, Lubensky TC, Janney PA. Nonlinear elasticity in biological gels. *Nature* 435: 191–194, 2005.
- Stossel TP, Condeelis J, Cooley L, Hartwig JH, Noegel A, Schleicher M, Shapiro SS. Filamins as integrators of cell mechanics and signaling. *Nature Reviews Molecular Cell Biology* 2: 138–145, 2001.
- Sunamoto M, Husain M, He JC, Schwartz EJ, Klotman PE. Critical role for Nef in HIV-1-induced podocyte dedifferentiation. *Kidney Int* 64: 1695–1701, 2003.
- Tseng Y, An KM, Esue O, Wirtz D. The bimodal role of filamin in controlling architecture and mechanics of f-actin networks. *J Biol Chem* 279: 1819–1826, 2004.
- Van der Flier A, Sonnenberg A. Structural and functional aspects of filamin. *Biochim Biophys Acta* 1538: 99–117, 2001.
- Yao J, Le C, Kos CH, Henderson JM, Allen PG, Allen BM, Denker BM, Pollak MR.  $\alpha$ -Actinin-4-mediated FSGS: an inherited kidney disease caused by an aggregated and rapidly degraded cytoskeletal protein. *PLoS Biology* 2: e167, 2004.
- Zhong J, Zuo Y, Ma J, Fogo AB, Jolicœur P, Ichikawa I, Matsusaka T. Expression of HIV-1 genes in podocytes alone can lead to the full spectrum of HIV-1-associated nephropathy. *Kidney Int* 68: 1048–1060, 2005.